Status and prospects of the JUNO experiment

IOP Conf. Series: Journal of Physics: Conf. Series **888** (2017) 012022 doi:10.1088/1742-6596/888/1/012022

Status and prospects of the JUNO experiment

Gioacchino Ranucci on behalf of the JUNO Collaboration

Istituto Nazionale di Fisica Nucleare
Via Celoria 16
20133 Milano - Italy

Gioacchino.ranucci@mi.infn.it

Abstract.

The JUNO (Jiangmen Underground Neutrino Observatory), a 20 kton multi-purpose underground liquid scintillator detector, has been proposed and approved for realization in the south of China. After an intense design phase, the overall concept of the structure of the detector has been finalized, paving the way towards the construction of the several components and subsystems, which will compose it. Meanwhile, the excavation of the site which will host the experiment has been started and is rapidly progressing. The main physics target of JUNO is the determination of the neutrino mass hierarchy, which will be accessible through the measurement of the antineutrino spectrum from two high power nuclear complexes under installation 53 km away from the experimental site. In this work, after the description of the broad physics capabilities of the experiment, which include in addition to the crucial measure of the neutrino hierarchy the high precision determination of three oscillation parameters, as well as a rich astroparticle program, I illustrate the technical characteristics of the detector, with particular emphasis on the technological challenges which are being addressed along the path towards its realization.

1. Introduction

The successful saga of neutrino oscillation, culminated in the 2015 Nobel Prize, paves the way to a future, rich and diverse experimental program of precision experiments tasked to complete the determination of the elements of the PNMS oscillation matrix with unprecedented accuracy, and to unravel the yet undiscovered features of neutrino properties. Therefore, mass hierarchy determination, octant of θ_{23}, violating δ_{cp} phase and improved precision of the mass-mixing parameters (mixing angles as well as squared mass differences), are the core of the ambitious worldwide neutrino oscillation program shaped for the forthcoming two decades, while at the same time the Dirac or Majorana nature of the neutrino mass term, together with its absolute value, will be probed by a suite of dedicated experiments.

In this global context, the JUNO detector [1] will play a central role on two aspects: the determination of mass hierarchy and the precise measurements of the solar oscillation parameters, i.e. Δm^2_{21}, $sin^2\theta_{12}$, as well as of the atmospheric squared mass difference Δm^2_{31}.

JUNO will be designed and realized as a huge liquid scintillator detector, therefore exploiting a mature and well proved technology, which has already provided fundamental contributions to the neutrino oscillation study through several implementations (Borexino [2], KamLAND [3], Daya Bay [4], Reno [5] and Double Chooz [6] being the most recent examples). It will base its measurements on the detection of the global antineutrino flux coming from the cores of two nearby nuclear complexes, Yangjiang and Taishan, located at about 53 km from the experimental site.

The program will be complemented by an ensemble of astroparticle physics measurements, which will significantly enhance the physics potential of JUNO.

Overall requirements, technical features and the current status of the experiment are thoroughly described in this work.

2. Summary of characteristics and of physics goals

JUNO will be a new member of the renowned, long tradition family of reactor neutrino experiments based on the scintillation technology, whose first well known example was the Savannah River experiment, with which Cowan and Reines revealed for the first time the (anti)neutrino particle.

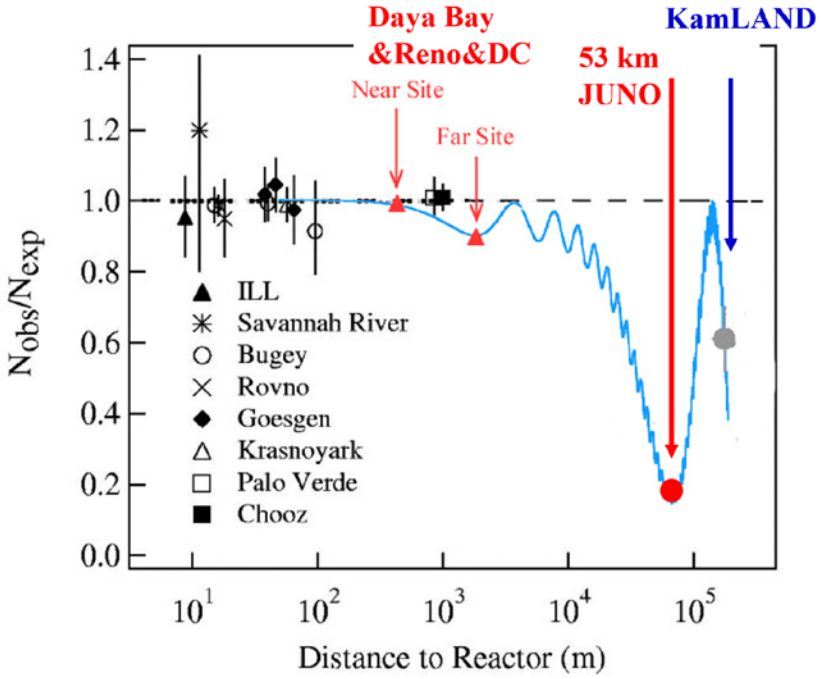

Fig. 1 – Summary of past reactors' results as ratio of observed to expected count rate, together with the predicted JUNO point

In Fig. 1 there is the summary of reactors' results accumulated so far, expressed as ratio of observed over expected events, contrasted with the prediction from the oscillation survival probability function. On the horizontal axis the reactor-detector distance is displayed; the plot reports the well-known fact that at small distance the impact of the oscillation phenomenon on the detector count rate is not visible, while it starts to manifest from roughly little less than 1 km baseline. At the special distance of 53 km the count rate suppression, mainly driven by the solar oscillation parameters, is maximal, therefore creating the best condition to study the interference effect governed in turn by the atmospheric mass squared difference, which is responsible for the ripple superimposed on the count rate suppressed profile. This is, therefore, the rationality beyond the choice of the optimum site and distance between JUNO and the emitting anti-neutrino cores.

To fully exploit this optimal baseline to perform an effective, and successful measurement of the mass hierarchy, the detector must be endowed with two essential characteristics: large mass to perform a high statistic measurements, and stringent energy resolution to clearly distinguish the ripple induced by the atmospheric mass squared term. The two key numbers in this respects are the total mass of 20 kton of liquid scintillator, and the energy resolution of 3% at 1 MeV, which represent, therefore, the major technical features which characterize the experiment.

In term of physics reach, such a high mass detector can tackle a plurality of measurements: beyond mass hierarchy and precision determination of neutrino oscillation parameters, it can provide fundamental results concerning many hot topics in the astroparticle field, like supernova burst neutrinos, diffuse supernova neutrinos, solar neutrinos, atmospheric neutrinos, geo-neutrinos, sterile neutrinos, nucleon decay, indirect dark matter search, as well as a number of additional exotic searches, as thoroughly illustrated in the physics program of the experiment (yellow book), published in [7].

3. Basic features of the program: detector structure, location and Collaboration

In terms of implementation characteristics, JUNO is a spherical unsegmented liquid scintillator detector that will push such a technology beyond the present limit, as far as the mass (20 kton) and the resolution (3%) are concerned. Succinctly, the detector can be described as a large spherical acrylic vessel, which will hold the scintillator volume, contained in turn in a water pool, to ensure adequate shielding against the gamma radiation and neutrons from the rock.

The vessel will be surrounded by a stainless steel truss which will perform the twofold task to sustain the vessel, by relieving its internal stress, and to provide the anchor support for the 18000 20” photomultipliers observing the scintillation photons. The light detection system will comprise also an additional set of 3” PMTs, up to 36000, which will be used for calibration purpose and to cross check the performances of the main PMTs, with the scope to control and reduce the systematic effects of the measurements performed by the main 20” PMT system.

Moreover, the shielding water around the acrylic vessel will be converted into a Cherenkov detector, being instrumented with about 2000 phototubes, which will detect the muon induced Cherenkov light. Such an arrangement, together with the top tracker that will be deployed on the roof of the detector itself, will allow an efficient muon veto capability, an essential feature at the planned shallow depth of the experiment, i.e. 700 m.

JUNO has been approved in China at the beginning of 2013 and has been later joined by groups from all over the world. Currently the Collaboration encompasses 66 institutions from Asia, Europe and America, with more than 450 researchers, and it is still expanding.

The experiment is located in the South of China, Guangdong province, Jianmeng County, Kaiping city, at 53 km from the two sites of Yangjian and Taishan, where 6 and 4 nuclear cores are planned, respectively. By 2020 according to the construction schedule of the plants 26.6 GW will be installed (2 cores will be missing at Taishan), while eventually the total power of 35.8 GW will be available.

4. How to infer the mass hierarchy

The observable quantity from which the mass hierarchy will be inferred is the positron spectrum detected in the liquid scintillator, stemming from the Inverse Beta Decay reaction through which antineutrino detection will occur. Specifically, the determination of the mass hierarchy relies on "inprinting" of the anti-ν_e survival probability on such spectrum.

The Inverse Beta Decay Reaction a là Cowan Reines is the following

$$\bar{\nu}_e + p \rightarrow e^+ + n$$

The energy deposited by the positron in the scintillator, i.e. its kinetic energy plus the total 1.022 keV energy of the two annihilation gammas, reflects faithfully the energy of the incoming anti-neutrinos

$$E_{vis}(e^+) = E(\nu) - 0.8\ MeV$$

$E_{vis}(e^+)$ is, thus, the specific measurement output to be analysed for the hierarchy evaluation.

The time coincidence (mean difference of the order of 250 μs) between the positron event and the γ ray from the subsequent neutron capture on protons allows to identify effectively the occurrence of neutrino detection and to pick up the positron scintillation signal, even in presence of uncorrelated background.

In order to describe the specific algorithm through which the MH can be unraveled, we resort to the electron (ant)neutrino survival probability, which in a full three flavor framework can be written as

$$P_{ee} = \left| \sum_{1}^{3} U_{ei} exp\left(-i \frac{m_i^2 L}{2E_i}\right) U_{ei}^* \right|^2$$

which explicitly becomes

$$P_{ee} = 1 - cos^4\theta_{13} sin^2 2\theta_{12} sin^2(\Delta_{21}) - cos^2\theta_{12} sin^2 2\theta_{13} sin^2(\Delta_{31}) - sin^2\theta_{12} sin^2 2\theta_{13} sin^2(\Delta_{32})$$

where

$$\Delta_{ij} \equiv \frac{\Delta m_{ij}^2 L}{4E_\nu}$$

In order to make the implication for mass hierarchy determination explicit, exploiting the approximation $\Delta m_{32}^2 \approx \Delta m_{31}^2$, P_{ee} can be written as:

$$P_{ee} = 1 - cos^4\theta_{13} sin^2 2\theta_{12} sin^2(\Delta_{21}) - sin^2\theta_{13} sin^2(|\Delta_{31}|) \\ - sin^2\theta_{12} sin^2 2\theta_{13} sin^2(\Delta_{21}) cos(2|\Delta_{31}|) \pm \frac{sin^2\theta_{12}}{2} sin^2 2\theta_{13} sin(2\Delta_{21}) sin(2|\Delta_{31}|)$$

The sign flip in front of the last term is due to the hierarchy: positive for direct hierarchy, negative for the inverse one. The presence of the multiplicative factor $sin^2 2\theta_{13}$ in this term questioned the effectiveness of this methodology, proposed for the first time in [8], until the experimental determination of the θ_{13} by Daya Bay, Reno and Double Chooz. Indeed, should θ_{13} have been resulted close to 0, the last term of the P_{ee} expression would have been vanishing small, making the proposed approach unfeasible. In reality, the discovery that θ_{13} is actually very close to the previous Chooz limit [9], opened the door to the actual implementation of the method.

The effect of P_{ee} on the reactor spectrum is shown in Fig. 2; the y axis is proportional to the event rate, while on the x axis the ratio L/E_ν is reported. The dashed line is the un-oscillated spectrum; the continuous black line is the spectrum distorted and suppressed as an effect of the "solar" oscillation: this large effect is the key for the very precise determination of the two "solar" mixing parameters Δm_{21}^2 and $sin^2\theta_{12}$.

The blue and red lines superimposed on the smooth black line, instead, display the effect of the interference term driven by the atmospheric mass squared difference. The frequency of the ripple depends on $|\Delta m_{31}^2|$ (which therefore can also be determined with high accuracy from the precise "tracking" of the ripple itself), while its phase is linked to the MH, as shown by the reciprocal shift of the blue and red lines in the figure. Unraveling the phase of the ripple, hence, is the clue for the MH determination.

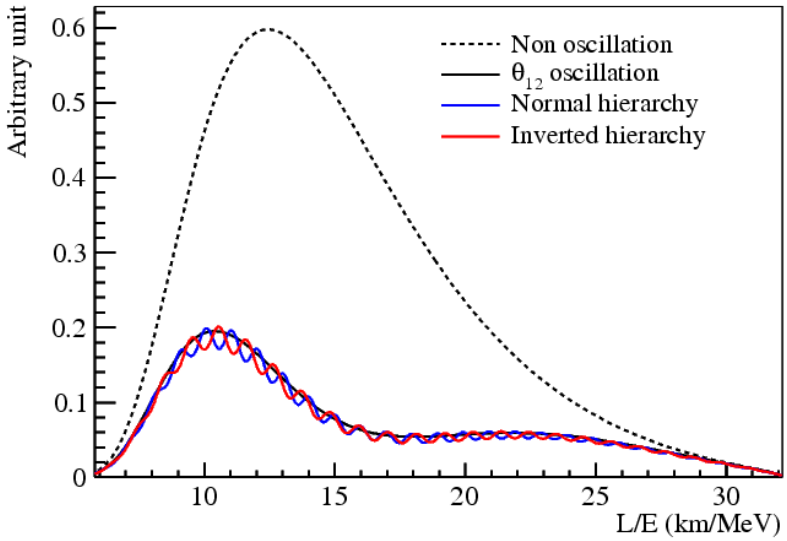

Fig. 2 - Effect of P_{ee} electron neutrino survival probability on the reactor spectrum

5. Resolution and sensitivity

The principle approach illustrated in the previous paragraph is characterized by a sensitivity that can be quantified in number of sigma's for ascertain the true hierarchy. However, in order to get a reasonable discovery capability, several experimental conditions have to be attained. In particular, as already highlighted, essential prerequisite to accomplish a meaningful experiment is the energy resolution. Why this experimental parameter is so important can be understood from Fig. 3: in the top part of the figure there is an ideal antineutrino spectrum computed for infinite resolution, in which the throats and peaks induced by the electron neutrino survival probability are perfectly visible.

On the other hand, in the bottom section of the figure it can be appreciated the positron visible spectrum, smeared by a 3%@1 MeV energy resolution, which clearly tends to smooth away the characteristic features of the ripple. However, at such a value of the resolution throats and peaks are still distinguishable and consequently the discrimination between the two hierarchies feasible. If, instead, the same exercise would be performed with 5 or 6% resolution, which are the values of the state of the art liquid scintillator technology of large scale experiments, peaks and throats would completely disappear, making any attempt to unravel the hierarchy impossible. From several numerical evaluations it stems that the 3% energy resolution considered in this exercise is just the limit value above which the hierarchy discrimination can be meaningfully performed and is therefore assumed as the design goal of the experiment, representing by far its greatest challenge in term of improvement over past experiences.

Concrete χ^2 calculations performed with the input parameters related to JUNO detector and site (i.e. baseline 53 km, fiducial volume 20 kt, thermal reactor power 36 GW, exposure time 6 years, proton content 12%, energy resolution 3%) indicate that the statistical discrimination power of the experiment amounts to a $\Delta\chi^2$ equal to 16 between the true and wrong hierarchy hypothesis.

However, if systematic effects are considered, there is unavoidably a loss of discrimination power. The most important effect in this sense is the non-exactly equal baselines from the nuclear cores to the experiment, characterized by a spread of about 500 m, which is responsible for a loss of 4 of the $\Delta\chi^2$ indicator. Other adverse effects detrimental to the discovery power are the 1% shape uncertainty of the reactor spectrum, and the background uncertainty (rate 4.5%, shape 0.35%). All in all, these effects bring the discrimination power down to $\Delta\chi^2 = 10.4$.

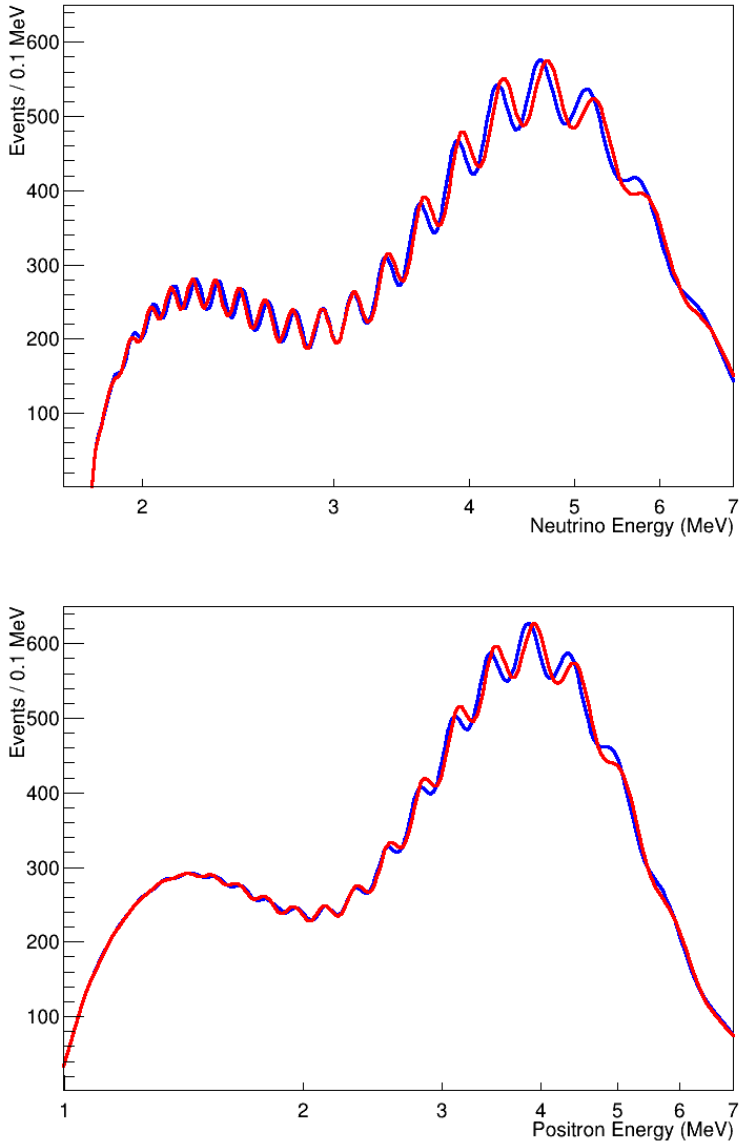

Fig. 3 –Top part: ideal antineutrino spectrum computed for infinite resolution; bottom: positron visible spectrum, smeared by a 3%@1 MeV energy resolution. In both plots normal and inverted hierarchies are considered

On the other hand, a recovery of this loss can be obtained including in the χ^2 analysis the a-priori information on the value of the atmospheric mass square difference, which will be available from the LBL experiments with 1% precision at the time of the JUNO data release. Such an information can be best incorporated through the effective mass square difference, $\Delta m^2_{\mu\mu}$, as defined in [10]. The net effect of this analysis approach is to recover a value of about 8 in the $\Delta\chi^2$, bringing back the discovery power of the experiment to the $\Delta\chi^2$=16 realm.

6. Precision measurement of oscillation parameters and other physics reaches

The huge effect of the survival probability on the reactor spectrum and the large amount of data that will be accumulated (JUNO plans to record 100000 events in 6 years of data taking) make it possible to

measure three of the mass-mixing parameters with unprecedented sub-percent precision: the two solar parameters Δm^2_{21} and $sin^2\theta_{12}$, and the effective parameter Δm^2_{ee} defined as (see [10]) $\Delta m^2_{ee} = cos^2\theta_{12}\Delta m^2_{31} + sin^2\theta_{12}\Delta m^2_{32}$.

From pure statistical considerations, the uncertainty of the measurements of these parameters is predicted to be very limited, i.e. 0.54%, 0.24% and 0.27% for $sin^2\theta_{12}$, Δm^2_{21} and Δm^2_{ee} respectively, taking also into account the correlation among them. Even adding background and several systematic effects, like the spectrum bin to bin uncertainty, 1%, the uncertainty on the absolute energy scale, 1%, and the energy non linearity, again 1%, the overall errors on the parameters remain below the 1% target: 0.67% for $sin^2\theta_{12}$, 0.59% for Δm^2_{21}, and 0.44% for Δm^2_{ee}.

For lack of space, I do not report here the results of many studies carried out to assess quantitatively the JUNO capabilities with respect to the several chapters of its vast astroparticle program, which are all illustrated in details in the already cited yellow book [7].

7. JUNO progress and schedule

The experiment is scheduled to start data taking in 2020. The ground breaking signaling the startup of the excavation occurred in January 2015. So far, more than half of the slope tunnel (900 out of 1340 m) and about half of the vertical shaft (300 out of 611 m) have been excavated. The former will allow to bring the scintillator underground, the latter will enable access of personnel and construction materials.

The civil construction is foreseen to be completed by about middle of 2018, including the large experimental hall. The preparation of the detector components, e.g. phototubes, acrylic panels, etc., has started in the current year 2016 and will encompass the whole 2017 and part of 2018, while the global onsite installation will be completed by the end of 2019. All this is in line to ensure scintillator fill and startup of data taking within the targeted 2020 year.

8. Main characteristics and features of the JUNO design

The basic configuration of the geometrical spherical structure of JUNO has been summarized in § 3 and is reported in Fig. 4. Few more information are added here.

The acrylic vessel containing the target scintillating volume is 12 cm thick and with an inner diameter of 35.4 m. The liquid scintillator will make use of LAB (Linear Alkyl Benzene) as solvent, in which two solutes will be dissolved, the scintillating PPO fluor (2,5-Diphenyloxazole), plus a wavelength shifter (bis-MSB).

The entire central detectors will sit in a pool 44.4 m high and 43.5 m of diameter, that will host also the purified shielding water.

On top of the detector several ancillary systems will be deployed, first of all a plastic tracker (recovered from the OPERA [11] experiment at Gran Sasso), which will select a pure sample of passing muons. Actually, the coverage will be partial, given the amount of sheets available, leading to the tracking of about 50% of the muons. This large sample will be contrasted with the corresponding signals from the central detector, to tune and optimize its muon tracking capability, in turn applicable also to the muon signals not tracked by the top tracker.

Moreover, the roof will accommodate also the equipment intended to deploy calibration sources within the scintillator volume, together with the filling and overflow systems to control the fill procedure, plus some electronics huts.

Key and distinctive feature of the central detector is the resolution, given its crucial role played for the feasibility of the mass hierarchy determination. From a pure statistical point of view the resolution is linked simply to the amount of registered photoelectrons, and therefore it can be easily determined that the required 3% at 1 MeV is obtained with a light yield of 1200 photoelectrons per MeV. The pre-requisite to reach such an unprecedented level of photoelectrons in a large liquid scintillator (as examples, KamLAND reached 250 pe/MeV, Daya Bay 160pe/MeV, and Borexino 500 pe/MeV the largest so far) is a vast coverage of the optical sensitive photocathodes. And indeed, the arrangement foreseen in JUNO is such to allow a coverage as high as 78% (large PMTs 75% and small PMTs 3%).

The coverage is the first of the ingredients needed for the light yield, the other two being the PMT quantum efficiency and the scintillator properties, both described later.

To quantify in a basic and clear approach the resolution characteristics and requirements of JUNO, we can resort to the following simplified relation

$$\frac{\sigma_E}{E} = \sqrt{\left(\frac{a}{\sqrt{E}}\right)^2 + b^2 + \left(\frac{c}{E}\right)^2}$$

where *a* represents the stochastic term governed via the overall maximization of light (i.e. through the mentioned coverage, PMT QE and features of the scintillator), and *b* and *c* are non stochastic terms controlled by the minimization of systematic effects. Such a control in the detector will be achieved in two ways, by an accurate calibration strategy and by the cross check measurements performed via the auxiliary system of the small 3" PMTs.

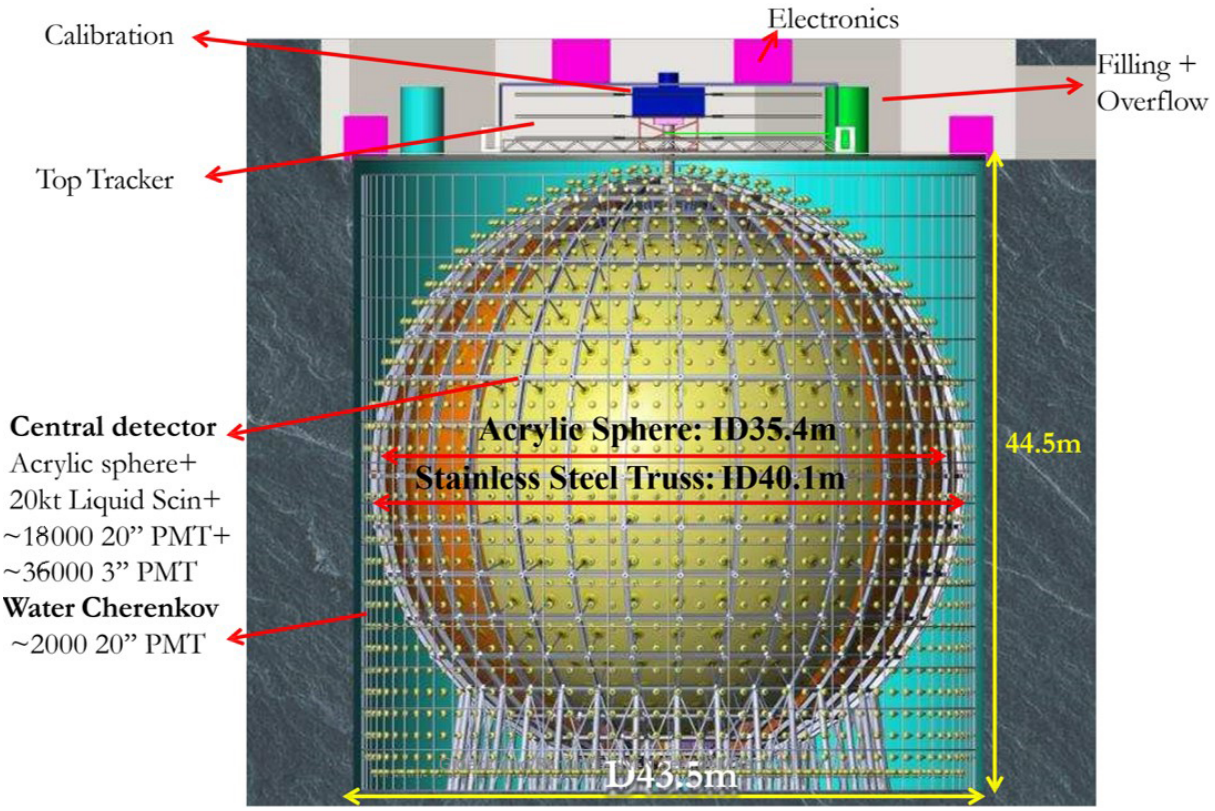

Fig. 4 – Schematic view of the JUNO configuration

The additional readout based on the 3" devices not only will help the main 20" PMT system to reach the 3% target in term of resolution, but will also ensure redundancy in several of the planned measurements of the experimental program. This is in particular valuable for the measurement of the oscillation parameters, the muon tracking needed to fight the cosmogenic background (^{9}Li, ^{8}He), and the supernova event detection. In general, the 3" PMTs will allow a full complementarity of the event identification, with particular emphasis on time resolution, spatial reconstruction, dynamic range and triggering strategy.

9. Progress of the subsystems

Several of the subsystems that will compose JUNO are in advance phase of design and preparation, following the tight schedule imposed by the goal to start data taking within 2020.

In this context the photomultipliers deserve a special mention as key elements for the construction and success of the experiment. The selection of the devices types was actually a recent important milestone achieved by the Collaboration, which decided to procure a combination of 5000 standard dynode-PMTs from Hamamatsu and of 15000 MCP-PMTs (i.e. with a Multi Channel Plate replacing the dynodes) from NNVT (North Night Vision Technology Co.,Ltd., Nanjing, a Company belonging to the NORINCO GROUP). Moreover, while the Hamamatsu PMT features the usual transmission photocathode, the NNVT device exhibits a combination of transmission and reflection cathode. With these two different solutions, both devices reach however the same specification value for the most critical parameter, the quantum efficiency which is guaranteed for both greater than 30%.

While for most of the other characteristics the two devices perform rather similarly, there are some differences, highlighting a complementarity between them which deserves to be emphasized. The first concerns the relative detection efficiency, which measures, on a relative basis, the overall capability of the device to develop a useful signal in response of an incoming photon: in this case the MCP tube performs 10% better than the dynode device. The second is the transit time spread, which contributes to determine the capability of vertex reconstruction of the detector: the Hamamatsu PMT features a 3ns (FWHM) performance, while the same quantity for the NNVT device is 12 ns. In practice, the 5000 Hamamatsu devices mounted in the detector will be enough to perform an accurate spatial reconstruction of the events.

Finally, the last difference between them concerns the radioactivity of the envelope, that for the Hamamatsu PMT is expected to be that of standard glasses, while for the NNVT a substantial reduction is foreseen.

The acrylic vessel is currently subject of a vigorous R&D effort. A tentative tessellation of the spherical geometry into more than 200 panels has been performed; moreover, several thermoforming attempts of the individual panels into the required spherical shape has been carried out in cooperation with three companies. The tests performed so far showed the capability of the potential suppliers to address positively the problems associated with the shape variation and shrinkage effect which unavoidably accompany the thermo-formation procedure.

Another hardware area that underwent through significant advancements since the beginning of the project is the read-out electronics. For this subsystems the Collaboration has opted for a very innovative and compact solution, in which the electronics boards are directly connected to the photomultiplier. As shown in Fig. 5, the base of the phototube will be enclosed by a potting shell filled with a combination of proper waterproof filling materials; several boards will be embedded within the filler, i.e. the voltage divider for the PMT, the readout electronics card and the associated power board. Overall, the entire tube-electronics assembly will be very compact, easing substantially the mounting procedure. Each optical unit will be completed by a twisted cable, a standard Ethernet (CAT5) cable, 100 long, that will bring the input low voltage down to the device and transmit the digitized signal of the phototube back to the external crates, containing the backend electronics.

The electronics card (GCU, global control unit) will host both the FLASH ADC chip, that will sample the PMT output, and a FPGA which will handle both command and data signals. Allocated on the divider board, there will be a HV Cockcroft-Walton unit which will multiply the low voltage input up to the value required by the proper operation of the tube.

This kind of design is very appealing in term of mechanical arrangement, but clearly requires a huge degree of reliability, since the underwater immersion of the assemblies will impede the access for maintenance and repair. For this reason a long term reliability test of about one hundreds of fully mounted prototypes will be performed before mass production.

The Cherenkov muon veto design will profit of the same solutions adopted for the central detector, phototubes and electronics, and therefore the main issue associated with its definition is the determination of the optimum installation procedure, which must be properly integrated with that of the central detector itself. In addition to this, a mechanical aspect to be considered for this subsystem is the

compensation for the magnetic field. The large cathode PMTs are unavoidably very sensitive to the Earth's magnetic field and therefore adequate shielding must be arranged. JUNO has decided for this purpose to use a global compensating scheme based on large Helmholtz coils surrounding the central detector, thus deployed in the region of the muon veto. Though not functionally involved in this part of the detector, their installation poses requirements to be addressed for the overall integration of the muon set up.

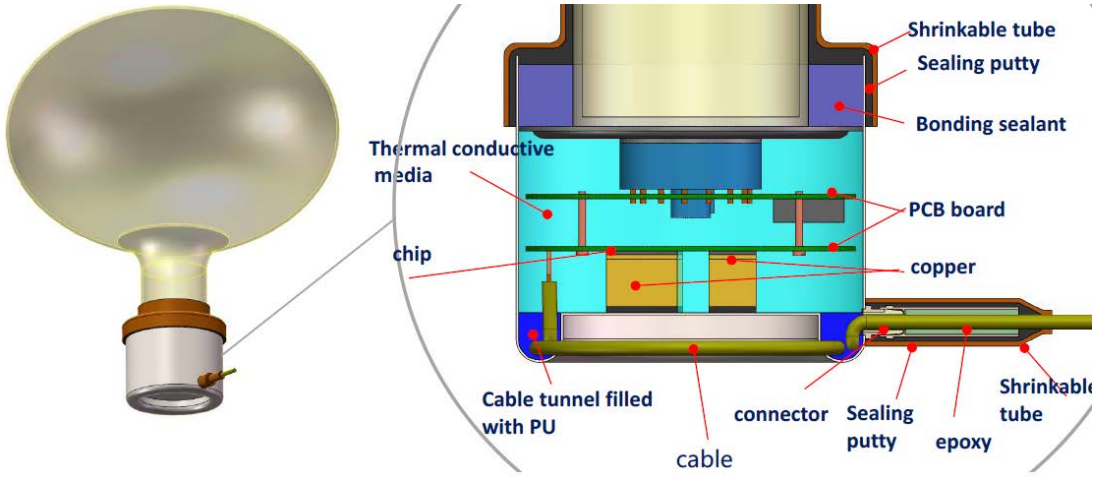

Fig. 5 – PMT with the base enclosed in the potting shell containing also the electronics

Concerning the other element constituting the muon veto, i.e. the top tracker composed by plastic sheets of scintillator, it has been decided that its modules will be accommodated in a three layer arrangement, which will ensure the optimum muon tracking. Both the supporting structure and the read-out electronics are in the phase of design and optimization.

Another subsystem undergoing a strong development effort is that formed by the plants for handling and purification of the liquid scintillator. The proper manipulation of the LAB is needed for two reasons: on one hand to ensure the degree of transparency which has to contribute to the overall light yield of the experiment, and on the other to keep the radiopurity of the liquid itself at least in the 10^{-15} g/g range (in term of U and Th contaminations) required for the mass hierarchy determination. Actually, the low energy neutrino measurements considered in the framework of the astroparticle program of JUNO require two order of magnitude better contamination, triggering a thorough purification effort of the scintillator which will employ several different means to try to achieve the needed 10^{-17} purity environment.

In this moment such a development is focused on the operation of a few pilot plants at the Day Bay site, where a combination of different methods is being tested to ascertain their effectiveness and suitability for the LAB purification. The techniques being evaluated comprise distillation, water extraction, absorption on alumina, and gas stripping. A complete test of the combined techniques will be performed in one of the anti-neutrino detectors of Daya Bay, whose scintillator will be replaced with the purified one to check globally the efficacy of the systems under evaluation.

Needless to say, all the other ancillary parts and equipment which will be incorporated in the final detector assembly, and will be pivotal for its operation, are being developed and designed, as well. In this list a prominent example is that of the calibration tools and sources, given their crucial role in assessing precision and accuracy of the critical energy scale parameter. Additionally, other vigorous activities are in progress for the electronics and ancillary part of the 3" PMT system, for the liquid scintillator filling equipment and procedure, for the overall slow control monitoring and control system, for the DAQ and the offline farms, and for the development of MC and analysis tools.

Finally, an important transversal effort which is encompassing the entire design of the detector is the radioactivity control of all the materials. A careful scrutiny of the construction elements, in addition to that focused on the liquid scintillator itself, is ongoing and will continue throughout the entire construction of the detector, with the purpose to control the global background rate to levels compatible not only with the mass hierarchy determination, but also with the entire astroparticle program.

10. Conclusion

The vast potential physics reach of very large liquid scintillator detectors, mass hierarchy determination and beyond, is the foundational motivation of JUNO conceived and planned to mark significant breakthroughs for the ultimate quest of the neutrino properties.

The Collaboration is rapidly progressing toward the construction of the detector with all the important design decisions already taken, the prototyping phase marking important steps forwards for all the subsystems and with the excavation of the site going ahead.

The JUNO exciting science program will start in 2020, when the experiment will be filled.

References

[1] T. Adam et al. (JUNO Collaboration), "The JUNO Conceptual Design Report", arXiv:1508.07166 (2016)
[2] G. Alimonti et al. (Borexino Collaboration), Nucl. Instr. and Meth and Meth. A 600, 568 (2009)
[3] S. Abe et al (KamLAND Collaboration), Phys. Rev. Lett. 100, 221803 (2008)
[4] F. P. An et al. (Daya Bay Collaboration), Phys. Rev. Lett. 108, 171803 (2012)
[5] J. K. Ahn et al., (RENO Collaboration), Phys. Rev. Lett. 108, 191802 (2012)
[6] S. Abe et al., (DOUBLE CHOOZ Collaboration), Phys. Lett. B, 723, 66 (2013)
[7] F. An et al. (JUNO Collaboration), J. of Phys. G (Nucl. and Part. Phys.) 43, id. 030401 (2016)
[8] S.T. Petcov and M. Piai, Physics Letters B 553, 94-106 (2002)
[9] M. Apollonio et al. (Chooz Collaboration), The European Physical Journal C 27, 331-374 (2003)
[10] H. Nunokawa, S. Parke, R. Zukanovich Funchal, Phys.Rev.D72, 013009 (2005)
[11] N. Agafonova et al. (OPERA Collaboration), Phys. Rev. Lett. 115, 121802 (2015)